

We are IntechOpen, the world's leading publisher of Open Access books Built by scientists, for scientists

6,900

Open access books available

185,000

International authors and editors

200M

Downloads

Our authors are among the

154

Countries delivered to

TOP 1%

most cited scientists

12.2%

Contributors from top 500 universities



WEB OF SCIENCE™

Selection of our books indexed in the Book Citation Index
in Web of Science™ Core Collection (BKCI)

Interested in publishing with us?
Contact book.department@intechopen.com

Numbers displayed above are based on latest data collected.
For more information visit www.intechopen.com



12-Pulse Active Rectifier for More Electric Aircraft Applications

Mohamad Taha

Additional information is available at the end of the chapter

<http://dx.doi.org/10.5772/intechopen.70882>

Abstract

The Aircraft industry is moving very quickly towards what it known as More Electric Aircraft (MEA). In a modern aircraft power technology system instead of using a fixed 400 Hz supply, a variable frequency supply (360 to 800 Hz) is used, which is dependent on the aircraft speed. In MEA electrical energy feeds the aircraft subsystems such as the flight control actuation, environmental control system, and utility function instead of mechanical, hydraulic and pneumatic energy. Although the new technology of MEA goes towards variable frequency supply, one of the essential parts of the power distribution systems require DC power sources to feed different DC loads, and a portion of load may require a fixed 400 Hz supply. This chapter simulation model of 12-pulse active rectifier for More Electric Aircraft applications.

Keywords: MEA, THD, active rectifier, boost converter, power factor, vector control

1. Introduction

Within the modern aircraft industry, More Electric Aircraft technology is growing rapidly. **Figure 1** shows a general block diagram for MEA power distributions. The power distribution system model consists of power generation unit, transformer rectifier unit, DC-DC converter unit, and DC-AC inverter unit.

The satisfactory performance of MEA depends to a very great degree on the continuing reliability of electrical systems and subsystems. This technology has many benefits and advantages such as:

- a. Decreasing maintenance and operating costs.
- b. Increasing dispatch reliability.
- c. Reducing gas emissions.

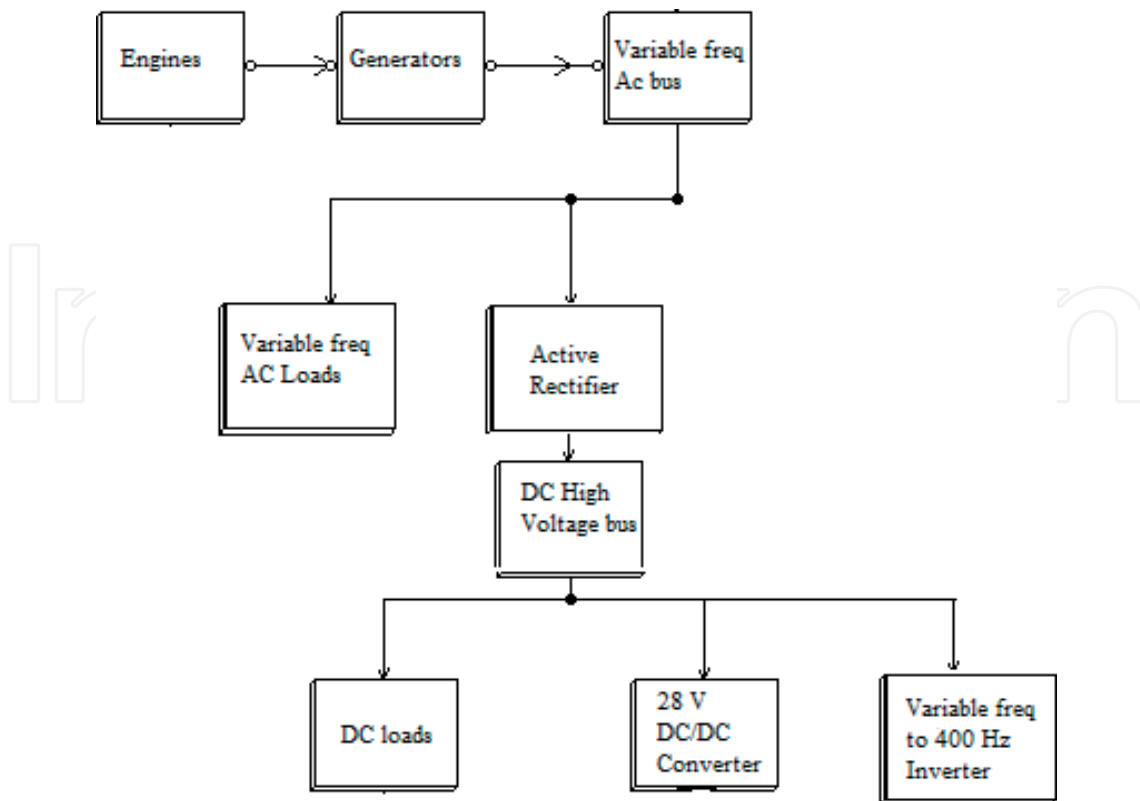


Figure 1. MEA general power distribution system.

In MEA Power Electronics segment plays a very important part in controlling the energy and improving both generators and actuators energy conversion. Furthermore, in a fixed frequency system (400 Hz) a mechanical constant speed drive set between the engine and the aircraft generator, however this will give extra weight and must be frequently maintained.

The use of Power Electronics helps in reducing weight, is easier to maintain, and provides more controllability and intelligence which includes fault detection and diagnosis [1–6].

A conventional 12 pulse rectifier using Diode Bridge is one of the simplest converter since does not require any control loop, however, this type of converter has a fixed DC output with high Total Harmonic Distortion (THD) on the input current compared with the proposed 12-pulse active rectifier.

The system has the ability to stabilize an output voltage of variable V_{dc} from a 3 phase 360–800 Hz, 115 V RMS system. Using a decoupling feed-forward control method by DQ frame technique, the magnitude and the phase of the input current can be controlled and hence the power transfer that occurs between the AC and DC sides can also be controlled. The converter could be suitable to use with an electric actuator (or other) aircraft loads. The system could be used as DC source for DC loads or to feed DC to AC inverter for a fixed 400 Hz supply. The design of this system poses significant challenges due to the nature of the load range and supply frequency variation and requires many features such as:

1. Sinusoidal and low harmonics contents on supply current.

2. High input power factor must be achieved to minimize reactive power requirements.
3. Power density must be maximized for minimum size and weight [7, 8].

Generally, use of electrical power on board is continuously increasing within the areas of communications, surveillance and general systems, such as: radar, cooling, landing gear or actuators systems. DC voltage of up to 540 V [9] may be required for electric power distribution to feed certain loads.

2. Harmonics and power factors for different rectifiers

Non-linear loads such as rectifiers can cause harmonics on the aircraft electrical supply systems, this will increase losses and can excite resonance in some circuits resulting in elevated voltages. For a resistive load, the harmonics current are proportional to the voltage harmonics. For a capacitive load the harmonics current will increase the capacitor heating and can cause premature failure.

For an inductive load harmonics increase losses in core components and also rotor losses in an induction motor will increase. Furthermore harmonics current could overheat transformers, therefore transformers, should be derated in the presence of harmonics.

In general rectifiers produce harmonics with the following order [10–14]:

$$h = \frac{f_h}{f_1} = K.P \pm 1 \quad (1)$$

where h = order of harmonics; f_h = frequency of the harmonic current; f_1 = fundamental frequency; P = rectifier pulse number; $K = 1, 2, 3, \dots$

The amplitude of the harmonic currents caused by rectifier can be calculated as:

$$I_h = \frac{I_1}{h} \quad (2)$$

where I_h = amplitude of harmonic current order; I_1 = amplitude of the fundamental current of the rectifier.

In AC power systems with pure sinusoidal voltage and current, the cosine of the phase difference (φ) between the voltage and current represents the power factor ($PF = \cos \varphi$). If the voltage or current waveforms contain harmonics, the phase angle between them is no longer represents the power factor. In general, the power factor could be calculated as [11].

$$PF = \frac{\text{mean power}}{V_{rms} I_{rms}} \quad (3)$$

Rectifiers draw non-sinusoidal current and have high harmonic components, however, if the input voltage of the rectifier is considered to be a pure sinusoidal, therefore the mean power will be:

$$P_{mean} = V_{rms} I_{1rms} \cos \varphi_1 \quad (4)$$

Therefore:

$$PF = \frac{I_{1rms}}{I_{rms}} \cos \varphi_1 \quad (5)$$

Where $\frac{I_{1rms}}{I_{rms}}$ is defined as the input distortion factor; I_{1rms} is the RMS value of the fundamental current; $\cos \varphi_1$ is the phase angle between the voltage and the fundamental current (input displacement factor).

Electronic devices in MEA technology are increasing, which are usually powered by switched mode power supplies (SMPS). SMPS will properly feed from a diode rectifier which imposes harmonic currents and possibly voltages onto the mains power network on the aircraft systems. This can cause some damage to the cables and equipment within the aircraft electric network. Supply current waveform may be expressed by the Fourier series [11–14]:

$$i_s(t) = I_{DC} + \sum_{n=1}^{\infty} (a_n \cos n\omega t + b_n \sin n\omega t) \quad (6)$$

For three phase 6-pulse diode bridge, the DC output voltage and the RMS input current equal:

$$V_{DC} = \frac{3\sqrt{3}}{\pi} V_m \quad (7)$$

V_m is the maximum phase voltage.

$$I_{RMS} = \frac{\sqrt{6}}{3} I_{DC} \quad (8)$$

Assume losses of the rectifier is zero, therefore the power is

$$P_{out} = P_{in} = V_{DC} I_{DC} = \frac{3\sqrt{3}}{\pi} V_m I_{DC} \quad (9)$$

The input apparent power for the rectifier is:

$$S_{in} = 3V_{RMS} I_{RMS} = \sqrt{3} V_m I_{DC} \quad (10)$$

Therefore:

$$PF = \frac{P_{in}}{S_{in}} = \frac{3}{\pi} = 0.955 \quad (11)$$

Although the power factor is good, the THD value is relatively high and could have a bad effect on the aircraft power systems. The RMS of the input fundamental current for three phase 6-pulse diode rectifier with an inductive load is well known and equals to:

$$I_{1RMS} = \frac{\sqrt{6}}{3} I_{DC} \quad (12)$$

$$THD = \frac{\sqrt{I_{RMS}^2 - I_{1RMS}^2}}{I_{1RMS}} = \frac{\sqrt{\pi^2 - 9}}{3} = 31.08\% \quad (13)$$

The THD could be reduced by using 12-pulse rectifier as shown in **Figure 2**.

12-pulse diode rectifier is fed from a three phase star connected transformer on the primary side, star and delta transformers on the secondary side. Each transformer on the secondary side feeds a three phase 6-pulse rectifier and they add together to form a 12-pulse rectifier, this configuration gives 30° of phase shift which gave harmonics cancellation. The turn ratio of the delta transformer must be multiplied by $\sqrt{3}$ factor in order to get the same voltage level, this illustrated in **Figure 3** [14].

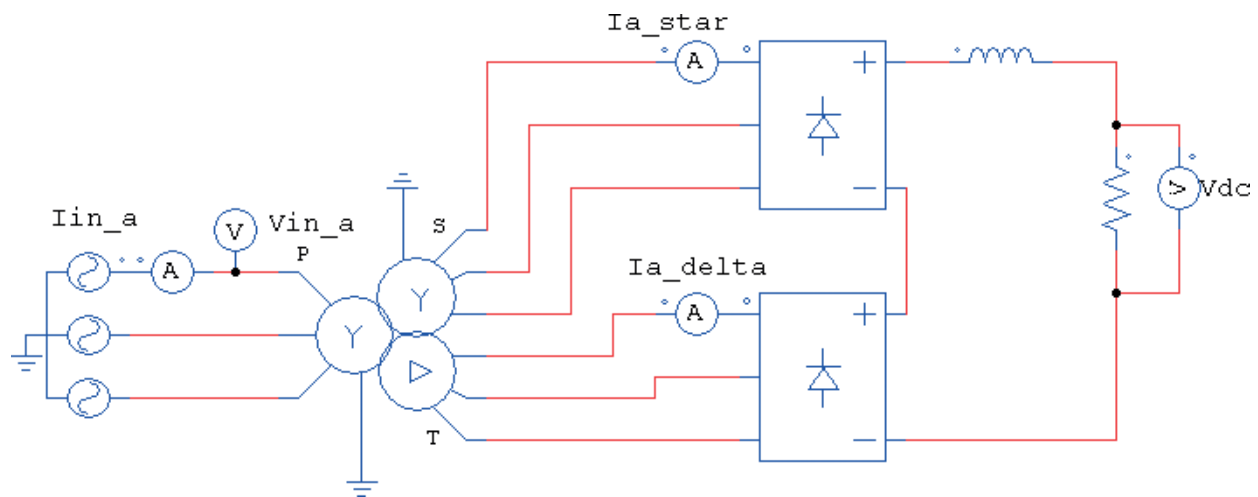


Figure 2. 12-pulse diode rectifier.

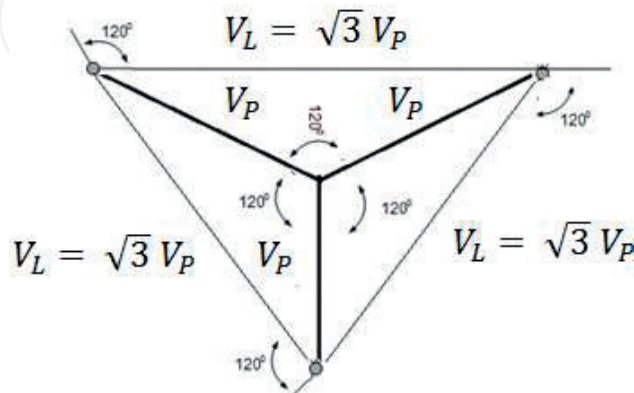


Figure 3. Star-delta configuration.

In a three phase 6-pulse rectifier the dominated harmonics are the 5th and 7th and this why THD is quite high. With a 12 pulse arrangement the 5th and 7th harmonics are canceled as illustrated below [11–14]:

For the star connection, phase (a) current equals:

$$i_{a_star}(t) = 2 \frac{\sqrt{3}}{\pi} I_d \left(\cos \omega t - \frac{1}{5} \cos 5\omega t + \frac{1}{7} \cos 7\omega t - \frac{1}{11} \cos 11\omega t + \dots \right) \quad (14)$$

For the delta connection phase (a) current equals:

$$i_{a_delta}(t) = 2 \frac{\sqrt{3}}{\pi} I_d \left(\cos \omega t + \frac{1}{5} \cos 5\omega t - \frac{1}{7} \cos 7\omega t + \frac{1}{11} \cos 11\omega t + \dots \right) \quad (15)$$

The primary current is equal to the summation of both secondary currents:

$$i_{a_inp}(t) = 4 \frac{\sqrt{3}}{\pi} I_d \left(\cos \omega t - \frac{1}{11} \cos 11\omega t + \frac{1}{13} \cos 13\omega t - \frac{1}{23} \cos 23\omega t + \dots \right) \quad (16)$$

The series has harmonics of an order of $12k \pm 1$ and the harmonics of orders $6k \pm 1$ circulate between the two converter transformers and do not penetrate the aircraft power system network. Since the magnitude of each harmonic is proportional to the reciprocal of the harmonic number, therefore the 12-pulse rectifier has a lower THD equals to:

$$I_{1RMS} = \frac{2\sqrt{6}}{3} I_{DC} \quad (17)$$

$$THD = \frac{\sqrt{I_{RMS(12h)}^2 - I_{1RMS(12h)}^2}}{I_{1RMS(12h)}} = 2 \frac{\sqrt{\pi^2 - 9}}{3} = 15.5\% \quad (18)$$

The THD for the 12-pulse rectifier is reduced by 50% compared with the 6-pulse rectifier.

Figure 4 shows the current waveforms for the supply input current of phase (a) and the currents on the secondary side of each transformer.

Figure 5 shows the harmonics contents for the currents of phase (a) and the currents on the secondary side of each transformer.

For a more THD reduction, 12-pulse active rectifier could be used, this is shown in **Figure 6**. Many advantages are associated with this type of converter:

- The power factor could be controlled by using DQ vectors control.
- THD is very low.
- The rectifier could be operated with a variable input frequency (usually 360–800 Hz) without interrupting its output.
- Bidirectional power flow.

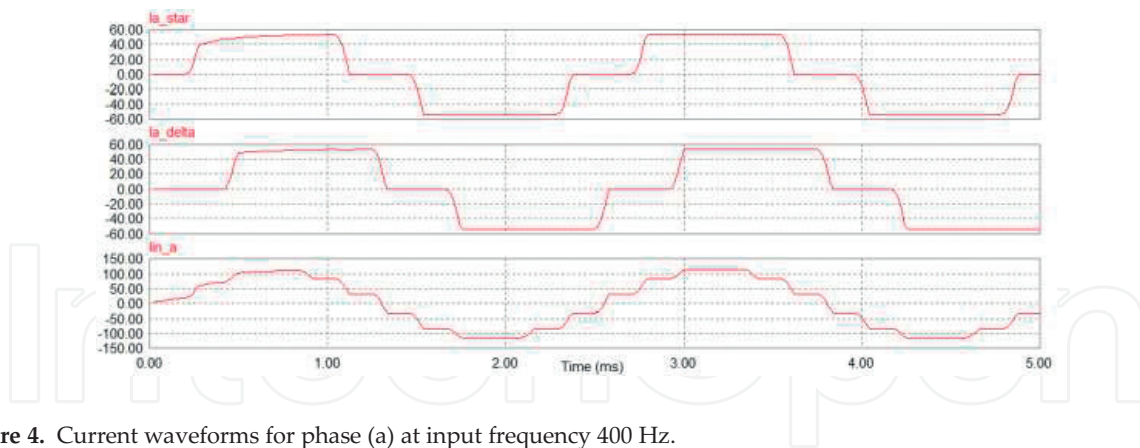


Figure 4. Current waveforms for phase (a) at input frequency 400 Hz.

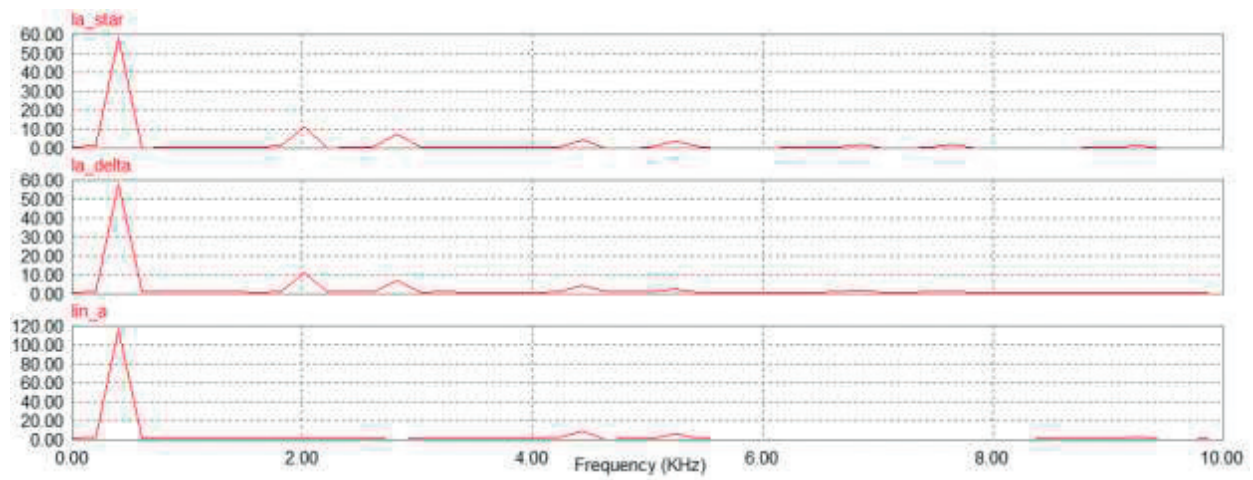


Figure 5. Harmonics contents for the currents of phase (a) at input frequency 400 Hz.

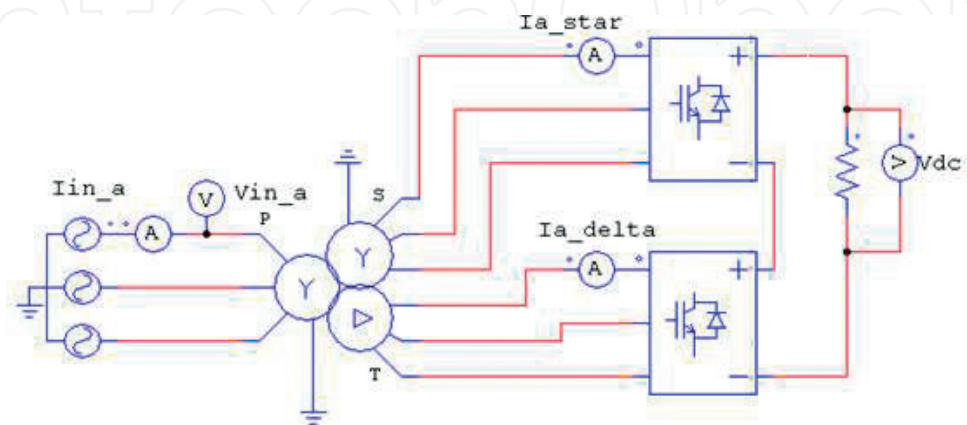


Figure 6. AC/DC 12 pulse boost converter.

3. DQ control circuit

Figure 7 show the configuration of the active rectifier for each secondary side.

The DQ transform is usually called Park transform which is a space vector transformation of the instantaneous 3 phase voltages and currents from a stationary phase coordinate system (ABC) to a rotating coordinate system (DQ) [7, 8].

The general formulas for DQ transformations are given as follows. We assume that the three-phase source voltages v_a , v_b and v_c are balanced and sinusoidal with an angular frequency ω .

The components of the input voltage phasor along the axes of a stationary orthogonal reference frame (α , β) are given by:

$$V_\alpha = \frac{2}{3}V_a - \frac{1}{3}V_b - \frac{1}{3}V_c \quad (19)$$

$$V_\beta = \frac{1}{\sqrt{3}}V_c - \frac{1}{\sqrt{3}}V_b \quad (20)$$

The input voltage can then be transformed to a rotating reference frame DQ chosen with the D axis aligned with the voltage phasor. The voltage components are given by:

$$v_d = V_\alpha \cos \omega t - V_\beta \sin \omega t \quad (21)$$

$$v_q = V_\alpha \sin \omega t + V_\beta \cos \omega t \quad (22)$$

The same transformations are applied to the phase currents:

$$i_d = I_\alpha \cos \omega t - I_\beta \sin \omega t \quad (23)$$

$$i_q = I_\alpha \sin \omega t + I_\beta \cos \omega t \quad (24)$$

Referring to **Figure 7**, let v_{a1} , v_{b1} and v_{c1} be the fundamental voltages per phase at the input of the converter.

$$v_a = Ri_a + L \cdot di_a/dt + v_{a1} \quad (25)$$

$$v_b = Ri_b + L \cdot di_b/dt + v_{b1} \quad (26)$$

$$v_c = Ri_c + L \cdot di_c/dt + v_{c1} \quad (27)$$

where L is the value of input line inductance and R is its resistance of the inductor.

Taking the DQ transformation for the inductor, the input voltage to the converter in the DQ reference frame is given by [15–19]:

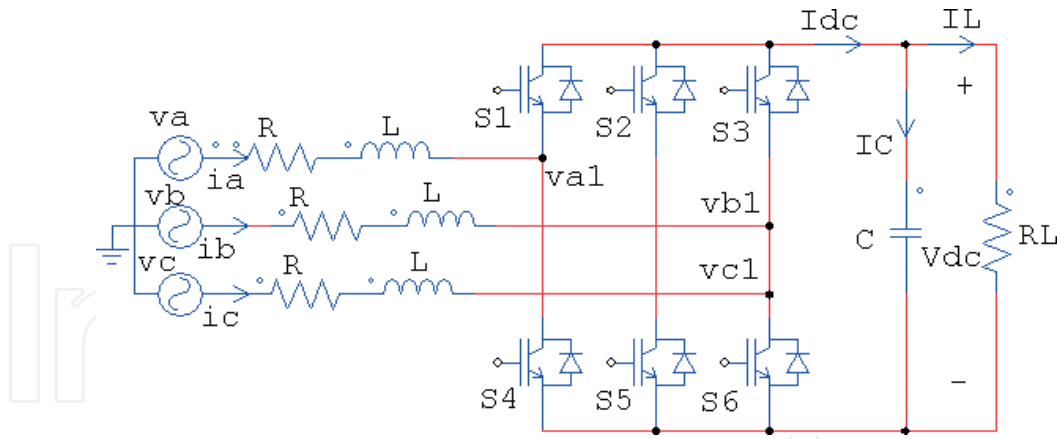


Figure 7. 6-pulse active rectifier configuration.

$$v_d = Ri_d + L \cdot di_d/dt - \omega Li_q + v_{d1} \quad (28)$$

$$v_q = Ri_q + L \cdot di_q/dt + \omega Li_d + v_{q1} \quad (29)$$

Note that v_{d1} and v_{q1} are the DQ components at the converter terminals.

Figure 8 shows the phasor diagrams for DQ coordinates.

The instantaneous active and reactive powers are given by:

$$P_d(t) = 3/2(v_d \cdot i_d + v_q i_q) \quad (30)$$

$$Q_d(t) = 3/2(v_d \cdot i_q + v_q i_d) \quad (31)$$

During the steady state and by assuming the converter losses are negligible, the DC and AC power are equal, therefore:

$$P_d = P_{DC} = V_{DC} \cdot I_{DC} \quad (32)$$

Therefore

$$I_{DC} = \frac{P_d}{V_{DC}} = \frac{3(v_d \cdot i_d + v_q i_q)}{2V_{DC}} \quad (33)$$

For a power balance, the delivering power should equal to the absorbing power therefore:

$$P_{AC} + P_{DC} + P_C = 0 \quad (34)$$

Where P_C is the power in the capacitor filter.

If the synchronous frame is aligned to voltage, the quadrature component, $v_q = 0$. Therefore, the power equations reduce to:

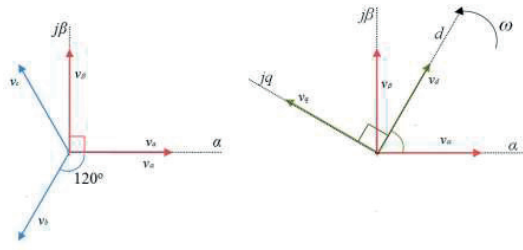


Figure 8. DQ phasor diagrams.

$$P_d = 3/2 v_d \cdot i_d \quad (35)$$

$$Q_d = 3/2 v_d \cdot i_q \quad (36)$$

Eq. (32) becomes:

$$I_{DC} = \frac{P_d}{V_{DC}} = \frac{3 (v_d \cdot i_d)}{2V_{DC}} \quad (37)$$

That gives:

$$P_{AC} + P_{DC} + P_C = 3/2 v_d \cdot i_d + V_{DC} \cdot I_{DC} + V_{DC} \cdot i_C = 0 \quad (38)$$

Therefore the capacitor current becomes:

$$i_C = - \left(\frac{3 (v_d \cdot i_d)}{2V_{DC}} + I_{DC} \right) \quad (39)$$

But:

$$i_C = C \frac{dV_{DC}}{dt} \quad (40)$$

From Eqs. (38)–(40):

$$\frac{dV_{DC}}{dt} = \frac{i_C}{C} = \frac{-1}{C} - \left(\frac{3 (V_d \cdot i_d)}{2V_{DC}} + I_{DC} \right) \quad (41)$$

From Eq. (41) by controlling the active Current i_d the DC output voltage of the rectifier could be controlled.

Inverse DQ transformations then need to be applied to provide the three phase modulating waves (v_{aref} , v_{bref} and v_{cref}) for the PWM generator. DQ vector control has several benefits such as reactive and active power will be easy to control and the dynamic response on the current loop will be very fast.

The PWM generator employs a 20 kHz carrier and is based on a regular asymmetric PWM strategy. The line inductor has a value of 100 μ H per phase which limits the Total Harmonic Distortion (THD) to the required value.

Figure 9 shows the schematic of the DQ control scheme implemented in the input converter.

The proposed control scheme consists of two parts [13–15]:

1. An outer voltage controller.
2. An inner current controller.

The outer voltage controller regulates the DC link voltage. The error signal is used as an input for the PI voltage controller this provides a reference to the D current of the inner current controller. **Figure 10** shows the DC link model and **Figure 11** shows the close loop control of outer voltage control.

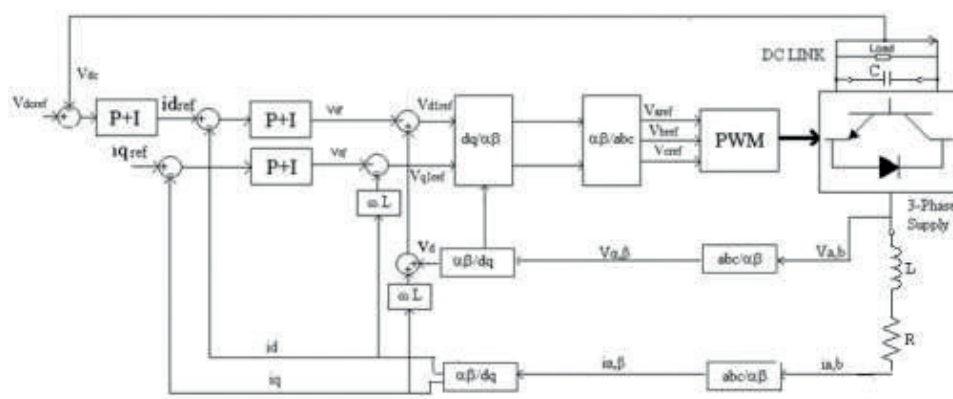


Figure 9. DQ control for the input converter.

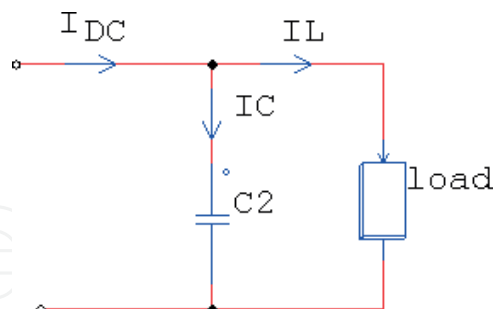


Figure 10. DC link model.

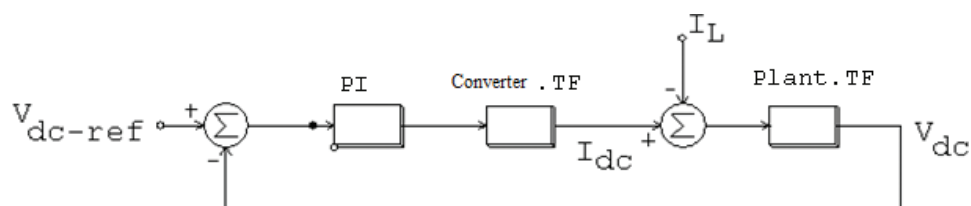


Figure 11. Close loop control of outer DC voltage control. PI TF: $K_p + K_i \frac{1}{s} = K_p \left(\frac{s + a_i}{s} \right)$; converter TF: $\frac{3}{2\sqrt{2}} M$; plant TF: $\frac{1}{Cs}$.

The relationship between the DC voltage and the D axis input voltage is given by:

$$V_{DC} = \frac{2\sqrt{2}V_d}{M} \text{ or } M = \frac{2\sqrt{2}V_d}{V_{DC}} \quad (42)$$

$$I_{DC} = \frac{3}{2\sqrt{2}} M I_d \quad (43)$$

Where: M is the modulation index.

For PI controller:

$$\text{PI TF} = K_p + K_i \frac{1}{s} = K_p \left(\frac{s + a_i}{s} \right) \quad (44)$$

Where $a_i = \frac{K_i}{K_p}$

For the converter the system has the following TF:

$$\text{Converter TF} = \frac{I_{DC}}{I_d} = \frac{3}{2\sqrt{2}} M \quad (45)$$

For the plant TF, The dc link may be modeled by a capacitor:

$$\text{Plant TF} = \frac{1}{Cs} \quad (46)$$

Therefore the characteristic equation for the DC link voltage control is given by:

$$s^2 + \frac{3MK_p}{2\sqrt{2}C} s + \frac{3MK_p a_i}{2\sqrt{2}C} = 0 \quad (47)$$

General equation for second order characteristic equation is given by:

$$s^2 + 2\xi\omega_n s + \omega_n^2 = 0 \quad (48)$$

Therefore the controller parameters are given by:

$$K_p = \frac{4\sqrt{2} C \xi \omega_n}{3M} \quad (49)$$

$$a_i = \frac{2\sqrt{2} C \omega_n^2}{3MK_p} \quad (50)$$

where ω_n and ξ are the closed loop natural frequency and damping ratio, therefore the controller parameters can be easily calculated by choosing the value of the modulation index, ω_n and ξ .

A PI inner DQ current control refers the phase current measurements to a rotating co-ordinate frame DQ fixed to the supply voltage. **Figure 12** shows the DQ model of input stage and **Figure 13** shows the close loop control of the inner current control. If the phase currents are in phase with the supply voltages, the current referred to the direct D axis becomes the DC link current and the current referred to the quadrature Q axis is equal to zero. The co-ordinate transformation is done using phase angle information derived from the measurement of the supply voltages. However, if the system is needed to operate with a leading or a lagging power factor, the Q axis reference value could be changed to define the displacement angle of the rectifier. The D axis and Q axis currents are compared to their respective demands values and the error is applied to individual PI controllers give voltage demands referred to D axis and Q axis. In the rotating co-ordinate frame the D axis and Q axis currents are inter-related due to their rotation. The rotation introduces an orthogonal component into time derivative of each current which, when applied to an inductive load, gives a voltage components along the axis orthogonal to that of the current. The DQ scheme studied uses two feed forward terms:

- $\omega L i_q$ fed into the V_d demand.
- $\omega L i_d$ fed into the V_q demand.

These feed forward terms de-couple the two currents. In addition the supply voltage is referred to D axis and this added to the V_d demand to avoid the integrator having to compensate for it. The final demand voltages are transferred back into stationary co-ordinates and the resulting sinusoids are used to generate the PWM.

Figure 13 shows the close loop control of inner current control. The following transfer functions are applied to the control block.

The plant is represent the line from the generator to the input of the converter which has RL network with following TF:

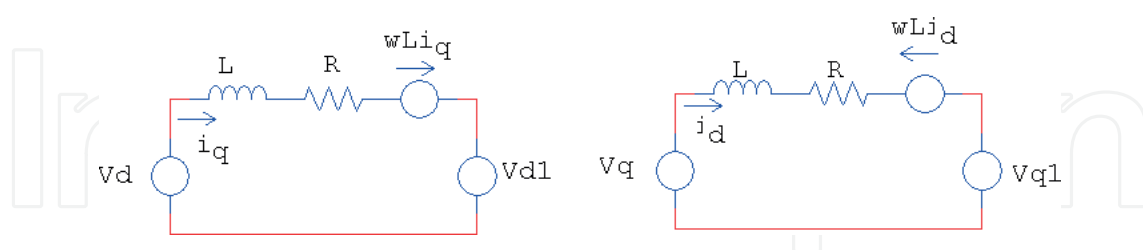


Figure 12. Equivalent circuit for DQ input supply.

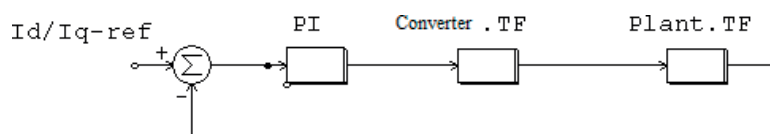


Figure 13. Close loop control of inner current control. PI TF: $K_p + K_i \frac{1}{s} = K_p (\frac{s + a_i}{s})$; converter TF: $\frac{1}{1 + T_s s}$; plant TF: $\frac{1}{R + Ls}$.

$$\text{Plant TF} = \frac{1}{R + LS} \quad (51)$$

The converter may be modeled as a first order lag. $= \frac{1}{1+Ts}$ where $T = \frac{1}{2F_s}$

F_s is the switching frequency. The same procedure can be used to calculate the parameters of the controller. Simulink or other tools can be easily used to tune the PI controller by using Zeigler-Nichol's method.

4. Simulation results for the 12-pulse active rectifier

In order to optimize the power quality and transient behavior of the power distribution system, a well-designed simulation model of the 12-pulse active rectifier based on detailed component models will be necessary.

For high voltage demand, the two rectifiers are connected in series, and for high current demand, the rectifiers may connect in parallel. The converter has been simulated for various operating conditions with the following parameters.

- Input inductance for $L = 100 \mu\text{H}$, input resistance 0.2Ω . For each converter
- DC filter $C = 200 \mu\text{F}$. For each converter
- Switching frequency 20 kHz . For each converter
- Input frequency $360\text{--}800 \text{ Hz}$.
- AC input voltage = 115 V RMS .
- Resistive load = 15Ω .
- The DC voltage reference for each converter is set to 320 V .

Simulation results show that comparing with a conventional 12-pulse diode rectifier, the low order harmonics are totally eliminated and only very low harmonics around the switching frequency at frequencies $f = mf_s$ where $m = 1, 2, \dots, \infty$

Figures 14–19 show different simulation results.

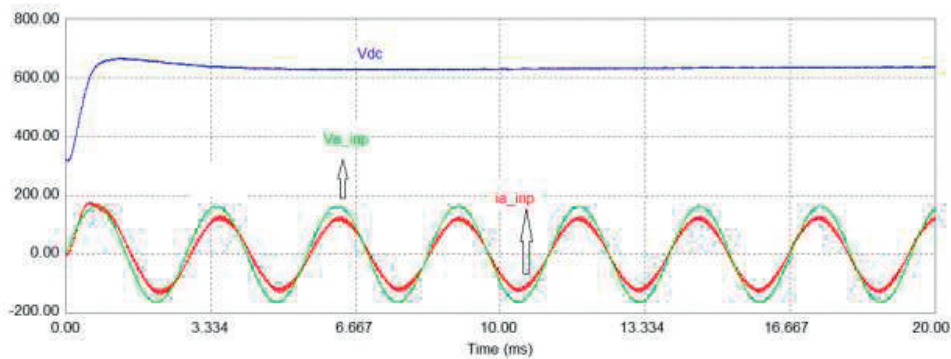


Figure 14. Waveforms results for 360 Hz input frequency.

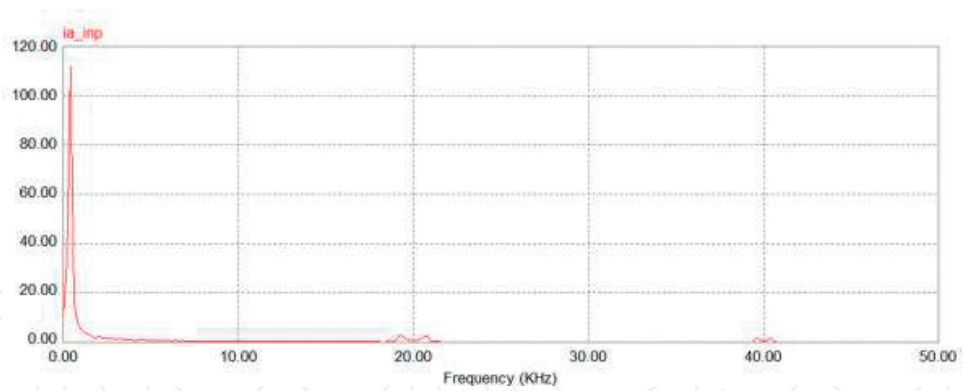


Figure 15. THD for phase a current—input frequency 360 Hz.

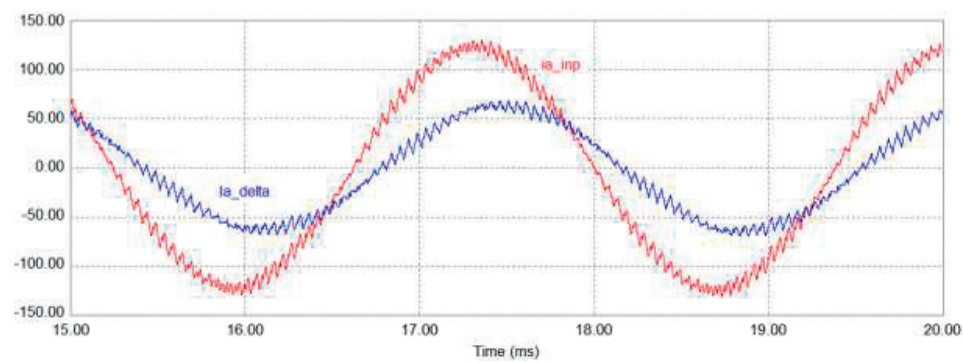


Figure 16. The 30° shift for the delta current and the input current for phase a—input frequency 360 Hz.

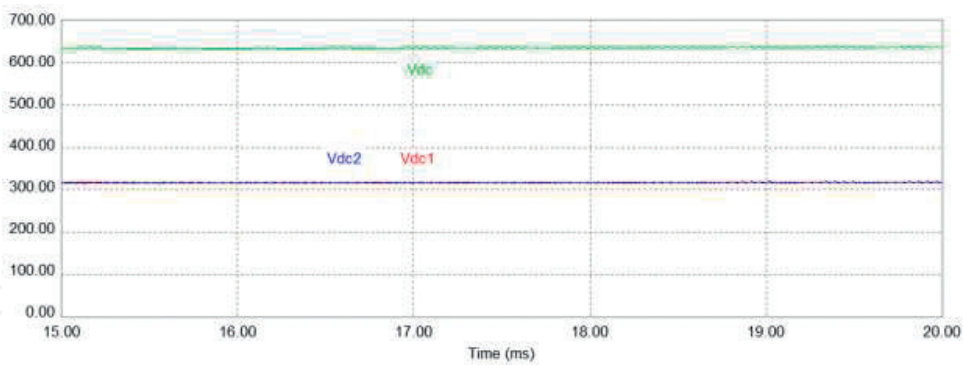


Figure 17. DC voltage level for each converter and the overall DC voltage.

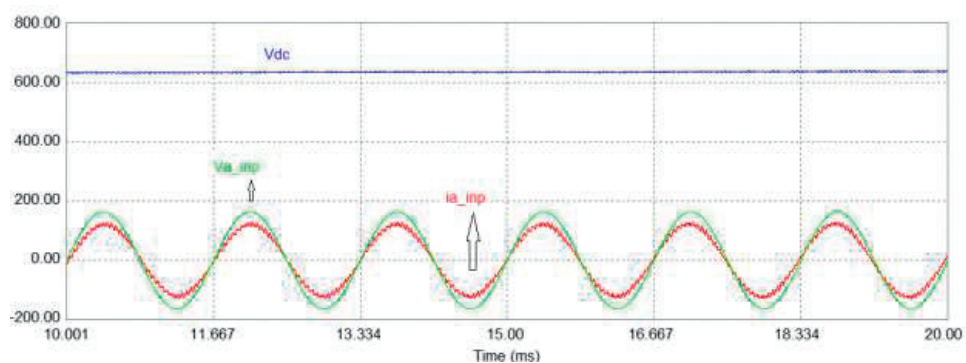


Figure 18. Waveforms results for 600 Hz input frequency.

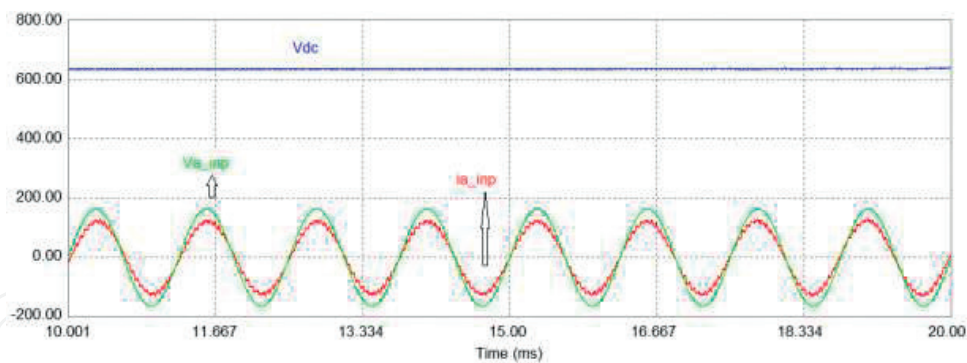


Figure 19. Waveforms results for 800 Hz input frequency.

5. Conclusions

With the future use of advanced power electronics the 12-pulse active rectifier gives a beneficial approach within the aircraft power distribution system. Any Low frequency current harmonics could be eliminated and there is the possibility to operate the rectifier at a variable power factor in order to provide system level benefits. Furthermore it has been shown that; there is the possibility to operate the system with variable input frequencies while keeping the input current harmonics low.

Acknowledgements

I would like to express my sincere appreciation and respect to the late Prime Minister Rafik Hariri who supported my studies in England.

Author details

Mohamad Taha

Address all correspondence to: tahamh@rhu.edu.lb

Rafik Hariri University, Lebanon

References

- [1] Faleiro L. Beyond the more electric aircraft. Aerospace America by the American Institute of Aeronautics and Astronautics. September 2005:35-40
- [2] Rosero JA, Orteg JA, Aldaba E, Romera L. Moving towards a more electric aircraft. IEEE A&E Systems Magazine. March 2007:3-9

- [3] Ahistrom K, Torin J. Future architecture of flight control systems. *IEEE A&E Systems Magazine*. Dec 2002;17(12):21-27
- [4] Faleiro L. Initial research towards a more electrical aircraft. In: *More Electrical Aircraft Conference Royal Aeronautics Society*; 2004. pp. 245-257
- [5] Wheeler P, Bozhko S. The More Electric Aircraft: Technology and challenges. *IEEE Electrification Magazine*. December. 2014;2(4):6-12
- [6] Sarlioglu B, Morris CT. More electric aircraft: Review, challenges, and opportunities for commercial transport aircraft. *IEEE Transactions on Transportation Electrification*. June 2015;1(1):54-64
- [7] Taha MH. Active rectifier using DQ vector control for aircraft power system. In: *IEMDC*; 2007. pp. 1306-1310
- [8] Taha MH, Skinne D, Gami S, Holme M, Raimondi G. Variable frequency to constant frequency converter (VFCF) for aircraft applications. In: *PEMD*; 2002. pp. 235-240
- [9] Guerreiro J, Pomilio A, Curi Busarello TD. Design and implementation of a multilevel active power filter for more electric aircraft variable frequency systems. In: *Power Electronics Conference, Brazilian*; 2013. pp. 1001-1007
- [10] Corcau JI, Dinca L. On using PEMFC for electrical power generation on more electric aircraft. *International Journal of Electronics and Electrical Engineering*. 2012;6(2):186-189
- [11] Prachi G. Effect of harmonics on active power flow and apparent power in the power system. *IOSR Journal of Electronics and Communication Engineering (IOSR-JECE)*:39-43. ISSN: 2278-2834, ISBN: 2278-8735
- [12] Almoataz YA. Sources and mitigation in harmonics in industrial electrical power systems: State of the art. *The Online Journal on Power and Energy Engineering (OJPEE)*. 2012;3(4):320-333
- [13] Sangeeta Sarali D, Shailaja P. Mitigation of harmonics using thyristor based 12 pulse voltage source PWM rectifier. *IJRET*. Nov 2012;1(3):267-271
- [14] Gong G, Drofenik U, Kolar JW. 12-pulse rectifier for more electric aircraft applications. In: *IEEE International Conference on Conference: Industrial Technology*; Dec 2003;2: 10-12
- [15] Faheme K, Chariac D, Sbita L. Control of three phase voltage source PWM rectifier. In: *3rd International Conference on Automation, Control, Engineering and Computer Science ACECS 16, Proceeding of Engineering and Technology (PET)*; 2016. pp. 649-654
- [16] Habetler TG. A space vector-based rectifier regulator for AC/DC/AC converters. *IEEE Transactions on Power Electronics*. 1993;8:30-36

- [17] Eid A, Abdel-Salam M, El-Kishky H, El-Mohandes T. Simulation and transient analysis of conventional and advanced aircraft electric power systems with harmonic mitigation. *Electric Power Systems Research*. Apr. 2009;**79**(4):660-668
- [18] Biagini V, Odavic M, Zanchetta P, Degano M, Bolognesi P. Improved dead of a shunt active filter for aircraft power systems. In: *Proc. IEEE ISIE*; Jul. 4-7, 2010. pp. 2702-2707
- [19] Kazmierkowski MP, Dzeiniakowski MA, Sulkowski W. Novel space vector based current control for PWM inverters. *IEEE Transactions on Power Electronics*. 1991;**6**:158-166